Hydride Transfer Tunneling-Ready-State Structure as a Function of Donor-Acceptor Distance: A Full Gating Coordinate for the Vibrational Tunneling-Ready-State

Nader Sakhaee[†]*, Edward Ackad[‡], and Yun Lu[†]*

[†] Department of Chemistry, Southern Illinois University Edwardsville, Edwardsville, IL 62025, USA

[‡] Department of Physics, Southern Illinois University Edwardsville, Edwardsville, IL 62025, USA

(yulu@siue.edu and nsakhae@siue.edu)

Abstract

The contemporary hydrogen-tunneling model involves a tunneling-ready-state (TRS) that is composed of activated structures of degenerate donor/acceptor (D/A) energies at various D-A distances (DADs). Current understanding of the DAD sampling over the gating coordinate is mainly from the observed temperature dependence of the 1º KIEs, which only suggests the broadness/narrowness of the sampling range. To better understand the gating coordinate of the TRS, computing TRS structures as a function of DAD is needed. Such computations have, however, been quite a challenge as in a real TRS the position of the hydrogen is uncertain and DAD is fluctuating. Using the self-exchange hydride transfer reaction from 2-propanol to protonated acetone as an example, an efficient set of dihedral angle restrictions in various initial activated donor/acceptor complexes were introduced to optimize to the TRS structures. The resulting gating coordinate suggests that the TRS could sample conformations of a wide range of DADs from 2.7 to 4.1 Å, with two major populations centered at around 2.9 and 3.9 Å, respectively. Zero-point energy, HOMO/LUMO energy, as well as the imaginary frequency for TRS structures, were calculated and their changes either along the H-tunneling coordinate or with the DAD were discussed to provide insight into the nature of H-tunneling.

Introduction

Quantum mechanical hydrogen tunneling has increasingly been accepted by the scientific community as a way to interpret the unusual kinetic isotope effects (KIE's) of H-transfers observed in solution and with enzymes.[1-7] The Bell H-tunneling model which adds a "simple" tunnel correction to the semi-classical transition state theory (TST) was the first to explain the primary (1°) KIEs and their temperature dependence which are outside of the semi-classical limits.[8] According to this model, temperature independence of 1° KIEs ought to be observed at very low temperatures, where the KIE is huge and the reaction rates of transfer for both isotopes are temperature independent.[9] However, temperature independent small 1° KIEs with temperature dependent rates were found in many H-transfer reactions at close to room temperature, especially in enzymes.[10-20] A motion assisted activated H-tunneling model, recently called the TST extension theory, and earlier vibrationally coupled H-tunneling model, were then proposed to explain such observations.[21-23] The latter models have two activation processes, both of which are assisted by heavy atom motions. One concerns the heavy atom reorganization coordinate ─ thermal energy is required to provide the energy needed for the reactants (Donor(D)-H and acceptor(A)) to reach an activated tunneling-ready-state (TRS) in which structure the reactant (D-$H^{\neq}$) and product (A-$H^{\neq}$) double potential wells are degenerate. This can occur at different donor-acceptor distances (DADs). The other concerns sampling of the DADs, i.e. the gating coordinate, thermal energy is needed to activate the skeletal vibrations so as to enhance DAD sampling for efficient Frank-Condon (FC) overlap and thus H-tunneling. This implicates a vibrational TRS. Figure 1 describes the gating coordinate, and shows the contribution of the sum of the FC overlaps at all DADs to the overall rate (Figure 1, left panel). This allows the H-tunneling coordinate to be separated from the overall activation process, isolating the temperature dependency of H-tunneling rates and thus 1° KIEs from the temperature dependency of the overall rate. Within this model, temperature dependency of 1° KIEs is ascribed to the temperature dependency of the DAD distributions. Temperature-independent 1° KIEs are ascribed to carefully organized TRS structures where the distribution of DADs is narrow, whereas the temperature dependent 1° KIEs come from the TRSs with a broader range of DADs. Note that this model has also been successfully used to explain the secondary (2°) KIEs on the basis of the former activation process that involves the overall structural change including rehybridization of the reaction centers.[5,7,24-27]

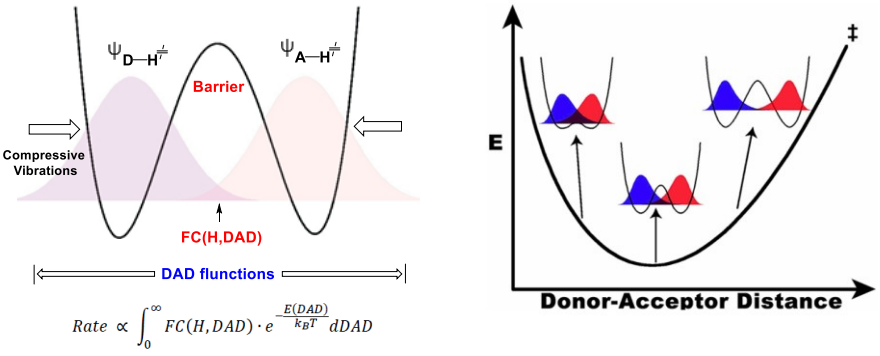

Figure 1. (Left) The DAD sampling activation process in the motion-assisted activated H-tunneling model (reprinted from our publication[26] with modification, copyright 2016 American Chemical Society). The H tunnels through the barrier in an activated TRS complex because of its wave nature. Once the H wave reaches the FC overlap area from the reactant (D-H$^{\neq}$) side, it can be found at the product (A-H$^{\neq}$) side. When the degeneracy of the double potential wells is broken, the H can be locked in the product well generating the product. The rate of the H-tunneling is directly proportional to the sum of the FC terms over all the DADs sampled; (Right) The presumed TRS energy vs. DAD diagram (reprinted form reference[28], copyright 2012 American Chemical Society)

Thus far, the H-tunneling coordinate (gating coordinate) is only qualitatively depicted as an assumed parabola shape in which the most populated DADs correspond to an ensemble of TRS structures of lower energy (Figure 1, right panel).[4,21,29] Understanding of the temperature dependence of 1° KIEs has been stagnant at a qualitative level with regard to the narrowness/broadness of the DAD sampling ranges on this coordinate. The structure and the vibrational nature of TRS are still unclear. While there has been no experimental methodology to determine the TRS structure and especially how it changes with DAD, theoretical computations may be possible to allow the computational replication of the experiments. This could provide information about the TRS and nature of H-tunneling. However, it is well known that optimization of a TRS structure is always challenging as the position of the transferring H is uncertain and the DAD is fluctuating. In this paper, an approach was developed to optimize various hydride-transfer TRS structures with different DADs, from a series of initial reactive complexes of different D-A distances. During the TRS/DAD optimization, certain dihedral angles were constrained in the initial complexes. Acquiring the TRS structures will help gain a theoretical insight into the nature of H-tunneling process as well as the gating coordinate. To the best of our knowledge this is the first computed "full" gating coordinate for a H-tunneling reaction.

The computation method and procedure are described using the hydride transfer reaction from isopropyl alcohol (**1**H) to the protonated acetone ($\mathbf{1}^+$) as an example (Scheme 1). The relationship among TRS structures, their potential energies and DADs are discussed and the gating coordinate is given. Furthermore, the detailed changes upon D-H$^{\neq}$ transitioning to A-H$^{\neq}$ in the TRS are, for the first time, discussed in terms of the changes in zero-point energy (ZPE) and HOMO/LUMO orbital energy. Further study is underway on the structural effects on the gating coordinate of the mixed systems. This method opens an avenue to possibly fit the observed 1° KIEs and their temperature dependency to the gating coordinate to find TRS structures for the general H-transfer reactions.

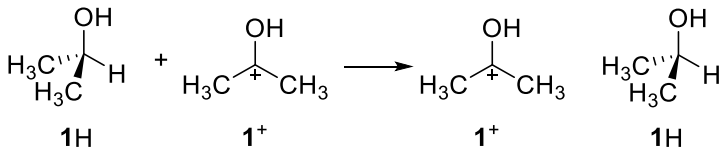

1H $\quad$ $\mathbf{1}^+$ $\quad$ $\mathbf{1}^+$ $\quad$ **1**H

Scheme 1: Hydride transfer reaction from isopropyl alcohol to the protonated acetone used as a prototype reaction to introduce the new approach to compute TRS's

Method development and Procedures

There have been attempts in literature to search for a method to find the vibrational TRS structures for H-tunneling reactions. Redington calculated such TRS structure for the intramolecular proton transfer in tropolone (**2**).[30,31]

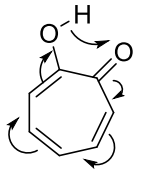

2

This method owes its success to the vibrationally assisted fluctuations in DAD because of the synchronous wagging mode of the C-O bonds.[32] This wagging mode accounts for the expected vibrational splitting and tunneling probability. In this system, DADs are sampled within a very narrow range. The method has, however, limitations for intermolecular H-transfer systems in which the donor and acceptor have more degrees of freedom and the DAD fluctuations have a potentially large range. Nevertheless, the method has been modified by freezing the donor-acceptor atoms at DADs longer than that in a classical TS in an attempt to find the TRS structures for intermolecular hydride transfer systems in both enzymes and solution.[25,26,33]

Note that the modified method looks for a linear [D-H$^{\neq}$---H-A$^{\neq}$] structure that has degenerate double potential wells so that the efficient H-tunneling (FC overlap) can occur (Figure 1, left panel). In that structure, the H appeared being "locked" in both wells. But in a real TRS it is delocalized in between the D and A. Therefore, the TRS was claimed to be a quantum superposition of the D-H$^{\neq}$ and A-H$^{\neq}$ states. It should also be stressed that this latter method has an already assumed DAD for a TRS in the restriction itself, and the fixed DAD facilitates the searching for the TRS.

In this paper we are seeking a different approach to find TRS structures for the intermolecular H-transfer systems, which would be to have an assumed initial D/A collision complex capable of optimizing to its own DAD for a TRS, rather than fixing the DAD beforehand. To compute a TRS with degenerate double potential wells, we first obtained an initial linear D---H---A complex geometry in which H is in the middle of the D and A, but not bonded to either. We then carried out a geometry optimization to find a TRS of certain DAD while applying the "linearity" and "H equidistant from D and A" constraints (Scheme 2). It is important to note that the main role of the "equidistant" constraint applied on the system is to find a TRS heavy atom framework so that the degeneracy of the double potential wells can be examined. Also note that the "linearity" property has been contained in the TRS obtained from the "frozen DAD" method. It has been shown that this ensures maximum H-tunneling through corner cutting and thus facilitates a tunneling mechanism.[34,35] Other quantum and molecular dynamic simulations also demonstrate that the D---H---A angle indeed does not substantially deviate from linearity.[36,37] Certain bond angles or dihedrals in the initial D---H---A complex were then constrained to optimize to a TRS structure of certain DAD. Note that in the sought TRS structure the D/A reacting atoms are still vibrating. This method thus entails a TRS of lower energy compared to that obtained from the "frozen DAD" method.

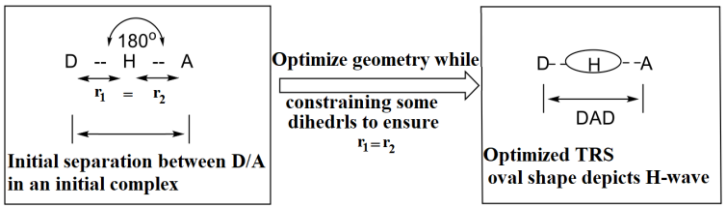

Scheme 2. Our strategy to search for a TRS of degenerate double potential wells. In the initial linear D---H---A complex, H is right in between D and A but not bonded to either. The initial complex is optimized to a TRS structure by freezing particular bond angles or dihedral angles. It has been found that the "frozen dihedral" method is more successful in generating the TRS structures than the "frozen bond angle" method (see text).

Below, we will use the simple self-exchange hydride transfer reaction between **1**H and $\mathbf{1}^+$ to describe our method and show that the "frozen dihedral" method gives TRS structures over a broad range of DADs.

The method development: from "frozen angle method" to the successful "fully-fledged frozen dihedral method"

A structure, in which the reacting donor carbon (C_D) and acceptor carbon (C_A) in **1H**/$\mathbf{1}^+$ are bonded without the transferring H, is first optimized in an attempt to obtain an assumed correlation between the D and A structures in a potential TRS structure. This preliminary structural correlation is a starting point toward computing a TRS structure. Two conformations with OH groups anti and gauche (syn) to each other (Scheme 3) were obtained and both conformations have similar energies. Then the two reacting carbons in each conformation are separated to a distance long enough for no apparent interaction. H is then placed right in between the C_D and C_A and is in line with them. The initial D/A complexes (syn and anti) have the geometries as follows,

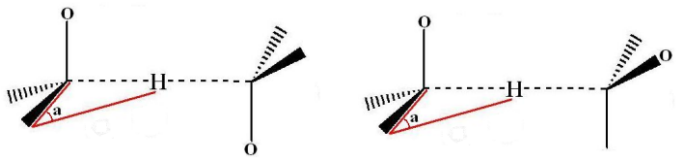

Anti **Syn**

Scheme 3. The syn and anti conformations of initial complexes for the isopropyl alcohol self-exchange reaction (Scheme 1). Indicated is the only angle type that helps successfully optimize to the TRS structures (see text and, *c.f.*, dihedral types in Scheme 4).

With the C_D---H---C_A and three other atoms bonded to each of the two carbons (a total of 7 atoms), there are many types of angles. We found that freezing all 6 angles with mouths opening towards C_D-H and C_A-H bonds (angle type *a* is shown in Scheme 3), together with the "linearity" constraint, could successfully optimize to a TRS structure with degenerate double potential wells. This geometry optimization process allows the DAD to vary, the D/A groups to rotate independently along the C_D---H---C_A axis, and the reaction centers to rehybridize. Separations between C_D and C_A from 3.0 to 6.5 Å in the initial anti and syn complexes were attempted. Some separations were found to give several TRS's with different DADs, whereas others did not successfully lead to a TRS. Therefore, this "frozen angle" method is not potent enough to

give TRS structures over a broad range of DADs and thus gives an informative gating coordinate.

On the other hand, in the initial geometries of anti and syn C_D---H---C_A complexes, we note that there are also different types of dihedral angles that we could possibly freeze to optimize the TRS structures. Following four (defined with the blue lines and colored planes in Scheme 4) are examples in the anti conformation. (One could rotate either side of the structure in any of these conformations to obtain the corresponding dihedral type for the syn conformation).

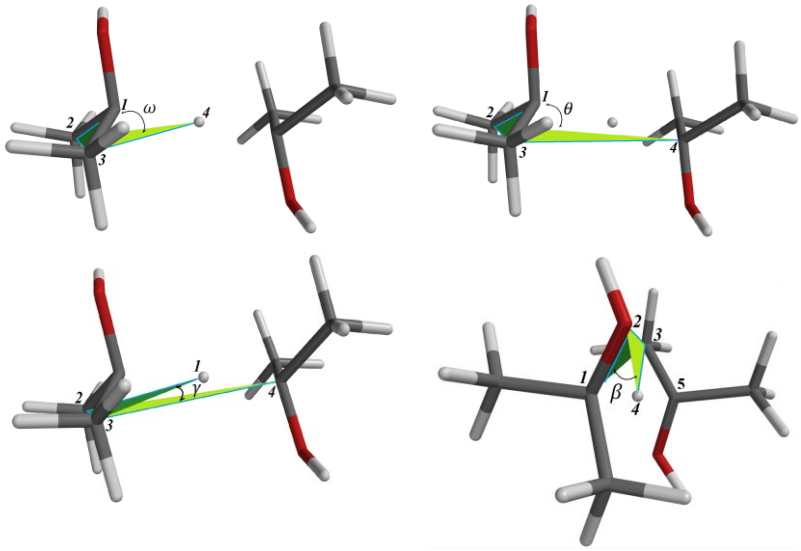

Scheme 4. The four dihedral types (θ, ω, γ, β) in the initial reactive complexes, freezing of which help successfully optimize to the TRS structures with different DADs. These dihedrals control $C_{A/D}$---H and C_A---C_D (DAD) distances during optimization (Note that the dihedral type ω parallels the angel type *a* in Scheme 3).

As compared to the frozen angle method, freezing the dihedrals (while still keeping the "linearity" constraint) is expected to impose less disturbance to the system in the optimization process (again through DAD change, independent rotation of donor acceptor groups around the D-H-A axis and rehybridization) and thus likely leading to lower energy TRS structures.

We attempted to freeze one type and a combination of two or three types of above dihedrals for optimization of the TRS. It was found that freezing one type or a combination of the two at a time worked, whereas freezing more either led to higher energy TRS structures or the optimization often failed. Thus, during an optimization one or two types of dihedrals were frozen while the remaining varied. It was further found that there exists a reasonable correlation between the change in the remaining dihedrals and the stability of the TRS structures on the

gating coordinate (see Figure 7 and corresponding discussion). Freezing ω, β separately, and combinations of $\omega\theta$, $\omega\beta$, $\omega\gamma$, $\gamma\beta$ and $\theta\beta$, yielded TRS structures of different DADs. Table 1 gives one such example with the initial D/A separation of 5 Å producing seven TRS structures both for the syn or anti conformation.

Changing the initial D-A separation will result in different dihedrals yielding TRS with different DADs upon optimization. Thus optimization of different initial D/A separation from 3.0 to 6.5 Å (with 0.5 Å increment in this work) (for both anti and syn) gave TRS structures spreading over a wide range of DADs. Table 2 listed selected TRS structures obtained from the optimization of various initial D---H---A complexes showing the broad distribution of DADs. A simplifying feature of this method is that most of the frozen dihedrals, or their combinations, work to optimize to the TRS structures, no matter what the initial conformation (anti or syn) or initial D/A separation is. This so-called "fully-fledged" frozen dihedral method is thus powerful enough to yield an ensemble of TRS structures over a broad range of DADs giving a potentially complete gating coordinate. Note that comparison of the TRS structures gained from this method with those from the frozen angle method showed that this approach indeed resulted in TRS of lower energies (by about 3-5 kcal/mol).

Table 1: The role of frozen dihedrals in determining the optimized DAD (More than one TRS structure (or DAD) were optimized from the same initial D---H---A complex for the **1**H/**1**$^+$ reaction) [a]

Initial Separation (Å)	Starting Conformation	Frozen Dihedral or its Combination	DAD (Å)
5.00	Syn	ω	2.659
5.00	Syn	β	2.865
5.00	Syn	$\omega\theta$	3.151
5.00	Syn	$\omega\beta$	3.431
5.00	Syn	$\omega\gamma$	3.521
5.00	Syn	$\theta\beta$	3.758
5.00	Syn	$\gamma\beta$	3.968
5.00	Anti	ω	2.688
5.00	Anti	β	2.867
5.00	Anti	$\omega\theta$	3.154
5.00	Anti	$\omega\beta$	3.433
5.00	Anti	$\omega\gamma$	3.583
5.00	Anti	$\theta\beta$	3.768
5.00	Anti	$\gamma\beta$	3.986

[a] Using the "frozen dihedral method"

Table 2: Combined effect of dihedral types and initial separations on the TRS structures of different DADs (optimized from different initial D---H---A complexes for the **1**H/**1**$^+$ reaction) [a]

Initial Separation (Å)	Starting Conformation	Dihedral Combination	DAD (Å)
3.50	Syn	$\omega\beta$	2.870
3.50	Anti	$\omega\beta$	2.919
4.00	Syn	$\gamma\beta$	3.295
4.00	Anti	$\gamma\beta$	3.316
4.50	Syn	$\theta\beta$	3.480
4.50	Anti	$\theta\beta$	3.490
5.00	Anti	$\omega\theta$	3.154
5.00	Syn	$\omega\theta$	3.131
5.50	Syn	$\omega\gamma$	3.777
5.50	Anti	$\omega\gamma$	3.867
6.00	Syn	$\theta\beta$	4.454
6.00	Anti	$\theta\beta$	4.459
6.50	Syn	$\gamma\beta$	5.035
6.50	Anti	$\gamma\beta$	5.130

[a] Using the "frozen dihedral method"

Imaginary frequencies of the TRS and calculation of the double potential wells

For each optimized structure, we generate the double potential wells to examine their degeneracy. In the "frozen DAD" method that Rosten and Kohen as well as our group previously used, the H position was scanned from the frozen D to A to produce the double potential wells.[25,26,33] In this work, we use another way to generate the double potential wells. We scan the structures along the coordinate of the imaginary frequency of the optimized TRS structure. In this way, the donor and acceptor reacting C's are vibrating while the position of the transferring H is scanned (Details can be seen in the section of Computational Methods below). For example, for an optimized structure of DAD = 3.154 Å when H is in the middle (Figure 2), there is a distinct imaginary frequency (1340 cm^{-1}) that reflects the H dynamics along the D-H-A axis. We thus scanned the structure along the coordinate of this imaginary frequency to generate the double potential wells for the particular TRS. The resulting corresponding degenerate double potential wells is included in Figure 2.

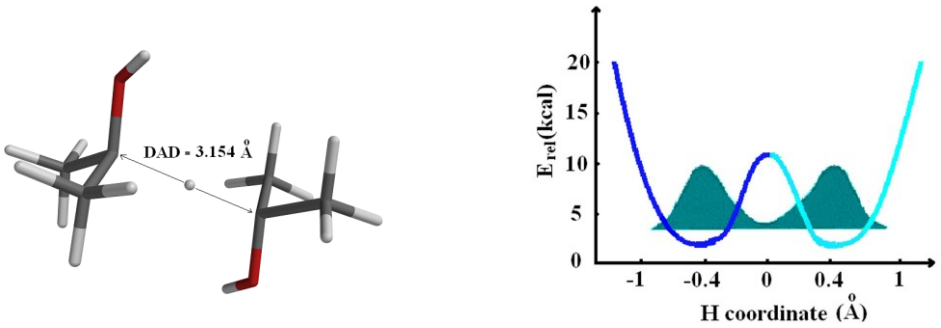

Figure 2. A TRS (left) optimized with the "Frozen Dihedral Method" from an initial anti D/A complex of 5 Å D/A separation and the corresponding degenerate double potential wells (right) for the reaction of **1H**/**1**$^+$ (obtained through scanning the structure along the coordinate of imaginary frequency, 1340 cm^{-1}, for the TRS structure shown). The numbers on the H-coordinate reflect the average position of the transferring H upon tunneling. The number 0 is chosen to emphasize the symmetry of the H-tunneling.

Computational Methods

All TRS structures were optimized using RM1 as a recently used effective level of theory for optimizing TRS structures.[38] We attempted to examine some of the structures using the DFT/B3LYP level of theory and 6-31+G* basis set. It was found that the obtained geometries were the same and only slight deviations of some C-H bond-lengths were observed.

Frequency calculations were included in all geometry optimizations (see *SI* Table S2 for a list of such frequencies for the TRS structure in Figure 2). The optimized TRS structure was scanned along the coordinate of the largest imaginary frequency to yield 40 structures reflecting the H transitioning from D-H$^{\neq}$ to A-H$^{\neq}$. These structures compose the so-called H-coordinate. The energy of each structure, relative to the lowest points of the degenerate double potential well, was plotted against the position of the H to give the degenerate double potential wells. The HOMO-LUMO energies were calculated (using the natural bond orbital (NBO) analysis method) to show the evolution of the molecular orbitals (MOs) along the H-coordinate, which gives a view how the electron is coupled with and thus drives the nucleus tunneling (Figure S2). The zero-point energies (ZPEs) of the TRS structures with H positioned differently at certain DADs were also obtained. Changes in dihedrals and their relevance to TRS stability at different DADs were examined and analyzed.

A 12 core Mac Pro equipped with Gaussian 09 and Spartan 14 as well as another 12 core Mac equipped with Spartan 10 were used to do single point energy computations and geometry

optimizations. Some of the DFT calculations were carried out using the facilities in the Pittsburgh supercomputing center using Gaussian 16 (see Acknowledgement).

Results and Discussion

Nature of hydride-tunneling

The change from $[C_D\text{-H}\text{---}C_A]^{\neq}$ to $[C_D\text{---H}\text{-}C_A]^{\neq}$ in the TRS could reflect the wave-like nature of the transferring H. Properties that can reflect such change may include the changes in imaginary frequency, ZPE and HOMO/LUMO energies during the H-tunneling in a TRS. They may be calculated from the respective TRS structures composing the double potential wells.

A. Imaginary frequencies

The frequencies of a structure are calculated using the harmonic approximation by calculating the eigenvalues which are related to the square of the frequency. Negative eigenvalues are thus imaginary frequencies and represent a repulsive force on the atom, breaking the harmonic approximation which assumes a restoring force ($F = -kx$). These vibrational modes represent atoms that are neither in the bottom of a potential well, nor at a saddle point of the potential energy surface, but instead in a classically forbidden region. This is expected for a TRS where the H is positioned within the tunneling barrier as a wave packet.

Using the *anti* TRS of DAD = 3.154 Å as an example, we examined the vibrational frequencies involved in the structure with H in the middle and found two imaginary frequencies, 1340 cm^{-1} and 116 cm^{-1} (Table S2). More such imaginary frequencies (up to four) start to appear as the DAD becomes longer. While the significant (largest) imaginary frequency for each structure reflects the maximum delocalization of the transferring H, *i.e.* the most diffuse wave packet, along the tunneling coordinate, other much smaller ones are most likely due to the independent rotation of the D/A groups around the D-H-A axis as well as other dynamics such as cofacial alignment of the D/A groups and two degenerate bending modes of the D-H-A axis (see Figure S3), which are expected to be more intense at longer DAD's. These are all signs of weaker D/A coupling for longer DAD's that tends to lead to collapse of the TRS dimer.

The significant imaginary frequency of each TRS structure of certain DAD along the H-coordinate was plotted against the H (or H-wave packet)-position. A bell-shape H-position dependence of the imaginary frequency was found, with its maximum value appearing when H is

equidistant from D and A. Figure 3 shows how sharply the imaginary frequency decreases as the H becomes correlated to one carbon more strongly than the other. When H is in the middle position it has the smallest association to the D/A thus having the maximum imaginary frequency (i_{max}) and suggesting the largest extent of H delocalization.

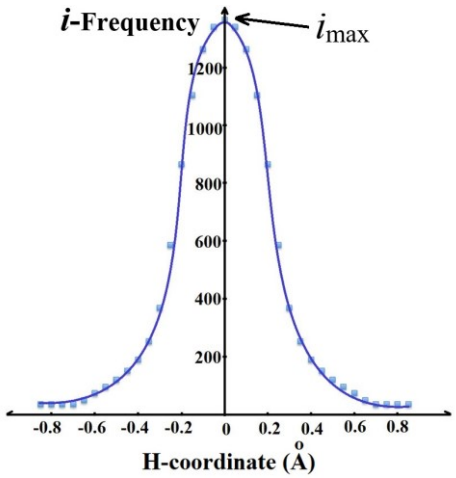

Figure 3. The H-position dependence of the significant imaginary frequencies (*i*-Frequency) along the H-coordinate for an anti TRS structure (DAD = 3.154 Å) (corresponding to the structure in Figure 2). The maximum imaginary frequency for a TRS of certain DAD is resulted from a structure in which the H is in the middle between D and A. It is represented by i_{max}.

The effect of DAD on the i_{max} of the TRS structure are listed in Table 3 (1st row). The i_{max} increases with DAD from 2.867 Å (i_{max} = 852 cm^{-1}) to 3.583 Å (2094 cm^{-1}), then has little change until 3.986 Å (2079 cm^{-1}), and then decreases (*e.g.*, 1365 cm^{-1} at 5.130 Å DAD). Note again that the larger the i_{max} is, the more delocalized the H as a wave packet would be. Therefore, results suggest that for the DAD change from 2.8 to 3.6 Å, the H wave becomes more and more delocalized (Figure 4 **A**-**C**). This is likely because the H wave packet tends to be more diffuse/delocalized at a longer DAD. There is, however, also a limit to such delocalization trend. At an even longer DAD the correlation between D/A and H decreases making the vibronic coupling between D and A less effective and thus decreasing the i_{max} value (also see Figure 4 and further explanations therein).

Table 3. Parameters reflecting the nature of H-tunneling in the *anti* TRS at different DADs for the **1H**/**1**$^+$ system

DAD (Å)	2.867	3.154 [a]	3.583	3.986	4.209	5.130
Maximum imaginary frequency (i_{max}, cm^{-1})	852	1340	2094	2079	1961	1365
Relative energy of HOMO (kcal/mol) [b]	-146	-118	-99	-82	-60	-25
HOMO-LUMO energy gap (kcal/mol) [c]	205	191	180	164	152	120

[a] Corresponding with the TRS structure in Figure 2; [b] relative to the non-bonding atomic orbital energies; [c] upon H-tunneling when the largest density of the H-wave is in the middle.

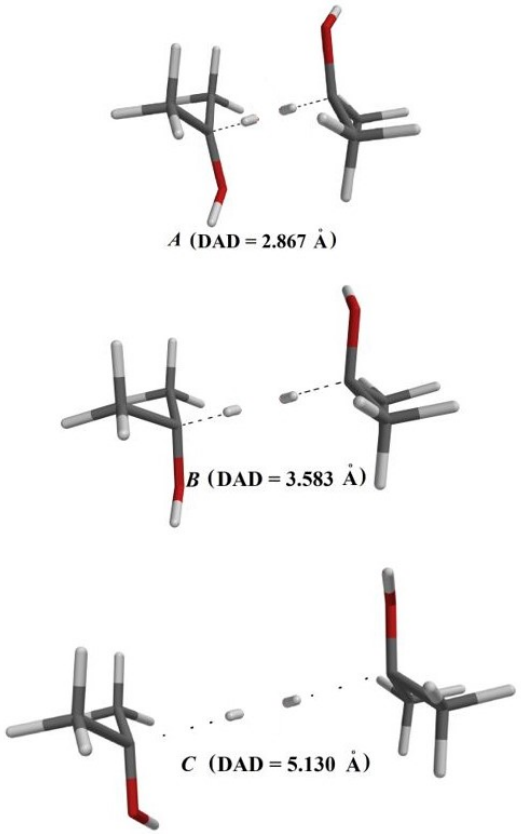

Figure 4. The effect of DAD on the maximum imaginary frequency (i_{max}) of the TRS structure. There are two effects. The first effect is the diffuseness of the wave packet, which increases with DAD from 2.867 to 3.583 Å. (From **A** to **B**, the wave packet becomes more diffuse, increasing the imaginary frequency value suggesting increasing wave property for the transferring H.) The second effect is the correlation between D/A and the transferring H, which decreases as DAD further increases from 3.583 to 5.130 Å. (The dotted line between D/A and H represents the correlation. The structure **C** has the weakest correlation, which means least effective vibronic coupling between D and A, thus having the lower i_{max} value than **B**.)

B. ZPE and HOMO/LUMO

The ZPE and HOMO/LUMO energies for each structure of the TRS along the H-coordinate were calculated (see *SI*). Figure 5 (top) shows the ZPE drop during the tunneling process in the *anti* TRS of 3.154 Å DAD (the structure in Figure 2). The ZPE drop is a fingerprint of the tunneling process, as reported previously for proton tunneling by Kiefer and Hynes.[39] It was attributed to the less attraction of the transferring H to the D/A reacting atoms.

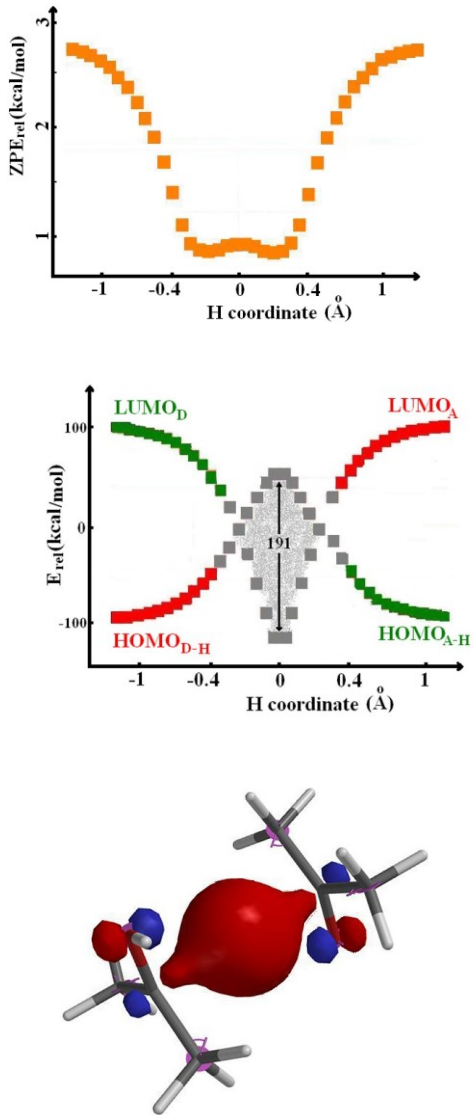

Figure 5. The nature of H-tunneling (D-H$^{\neq}$---A is transitioning to D---H-A$^{\neq}$) in an anti TRS for the **1H**/**1**$^+$ reaction (DAD = 3.154 Å) (See its degenerate double potential wells in Figure 2): (Top) The ZPE drop is a fingerprint of tunneling process.[39] (Middle) The change of HOMO/LUMO in reactants (D-H/A$^+$, in red) and products (D$^+$/A-H, in green), and the HOMO/LUMO identity exchange. The grey area is an avoided crossing area in which the HOMO/LUMO orbitals from D and A switch. Upon H-tunneling, HOMO in D-H becomes LUMO in D$^+$ and LUMO in A$^+$ becomes HOMO in A-H. The upright double-headed arrow indicates the HOMO/LUMO energy gap upon H-tunneling in the TRS. (Bottom) the HOMO orbital upon tunneling, chosen on the basis of symmetry consideration when H is in the middle. (see *SI* Figure S2 for HOMO evolution in a complete H-coordinate scan).

Figure 5 also includes the HOMO/LUMO energy change, their identity exchange in the avoided crossing region (grey color, middle), and the HOMO orbital upon H-tunneling in a TRS where the largest density of the H-wave is in the middle (bottom). Relevant data including the HOMO energy and the HOMO-LUMO energy gap upon H-tunneling are listed in the Table 3 as well. Note again that in all these properties calculated when scanning the structure along the coordinate of imaginary frequency, the transferring H was still treated as having a Born-Oppenheimer nucleus, but since in a real TRS structure the H is delocalized upon tunneling, its position is best thought of as $<x>_H$, *i.e.* a wave packet.

The changes in ZPE and HOMO/LUMO energy upon H-tunneling correspond with the change from $[C_D\text{-H---}C_A]^{\neq}$ transitioning to $[C_D\text{---H-}C_A]^{\neq}$ in the TRS (Figure 5). During the transition, the tunneling H's wave function spreads over the two wells of a degenerate double potential well. This reflects a pronounced wave-like property of the transferring H. During tunneling, the transferring H has the weakest correlation with D/A reacting atoms; therefore, the ZPE is the lowest. On the other hand, since the transferring H has a weaker interaction with D/A at a longer DAD, an increase in DAD is expected to be accompanied by an increase in the HOMO energy, and a decrease in HOMO-LUMO energy gap. These are consistent with the data in Table 3 (2^{nd} and 3^{rd} rows).

Gating coordinate – what does it look like?

The fully fledged frozen dihedral method allowed us to generate TRS structures over a range of DADs from 2.7 to 5.1 Å for the **1**H/**1**$^+$ reaction, from both the initial anti and syn D/A complexes of various D/A separations. Plots of the energies of the respective anti and syn TRS's *vs.* DAD are given in Figure 6. The anti TRS is found to be of slightly lower energy than the syn structure, and the energies of both structures change with DAD with the similar trend, giving similar gating coordinate. Therefore, the reaction would have two conformations of TRS's, anti and syn, both of which have very similar way of sampling of their DADs and thus the similar gating coordinate. The possibility of interconversion between the two types of TRS's appears unlikely, yet we have no clear way of distinguishing these, mainly due to the quantum nature of the process. The exemplified double potential wells placed over the plots are used to show the H-coordinate having different distance, energy, as well as barrier height for H-tunneling.

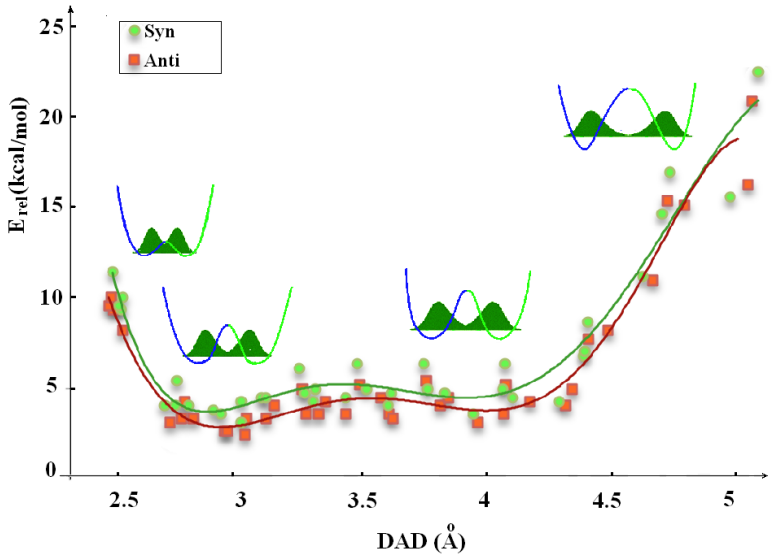

Figure 6. A diverse group of TRS structures obtained for the reaction of **1H**/**1**$^+$ from the fully-fledged frozen dihedral method. The energy refers to the minimum point energy of the degenerate double potential wells for each TRS (the double potential wells above the plots are used to represent the H-coordinate showing different tunneling distance, energy as well as barrier height).

It should be noted that using the different initial D/A complexes with D/A separation longer than about 3.0 Å did not give optimized TRS's having DADs shorter than 2.7 Å which are expected to have higher energies. In order to obtain the leftmost data points of the gating coordinate predicted in Figure 1 (right panel), we attempted to have the "initial D/A complex" of much shorter D/A separation such as 2.0 Å. Unlike the large separations, the D/A in these D/A complexes repelled each other optimizing to a cluster of TRS's of DADs at around 2.5 Å from freezing different dihedrals. (Note that here we used the same dihedral constraints to search for the TRS's).

One important finding from the gating coordinate is the clustered distribution of the TRS structures along the DAD coordinate (for both anti and syn) (see SI Figure S1). Such change in TRS structures could be a result of the DAD fluctuations on the gating coordinate.

A close examination of the TRS optimization results reveals that although the D/A separations in the chosen anti or syn initial complexes were evenly spaced with 0.5 Å increment for a large range of initial separations (3.0 – 6.5 Å), the resulting TRS's were not evenly distributed along the entire DAD range, but were rather clustered around certain DADs. Namely, each initial separation gave TRS structures at different DADs through freezing different dihedrals (*c.f.* Tables 1 and 2 for examples) and some other separations gave the TRS structures

at the similar DAD's to group as a cluster (see *SI* Figure S1 and Table S1 for cluster examples). The gating coordinate in Figure 6 is thus resulted from many such clusters at different DAD ranges. We then averaged the corresponding dihedrals of each cluster of TRS structures that would have similar conformations (anti and syn, respectively), and plotted them against their average DADs (Figure. 7 and see *SI* Table S1 for examples). Results show that all four dihedrals in both the syn and anti TRS structures have small changes within the DAD range from 3.0 to 4.0 Å, but θ and ω change greatly for DADs below 3.0 Å, suggesting that the R/A groups in the TRS rotate the most at the shorter DAD fluctuations. This is because there are more torsional strain at shorter DADs so that the rotation is needed to release part of it. Importantly, the results also show that the fluctuating pattern of the dihedrals with DAD correlates with the pattern in the TRS energy plot (Figure 6), *i.e.*, either maxima or minima of the dihedral ─ DAD plot (Figure 7) corresponds with the TRS of the lowest or highest energy as shown in the gating coordinate (Figure 6). This suggests that not only these dihedrals help optimizing the TRS structures, but they are also quite crucial in determining the stability of the resulting TRS structures. It should be noted that D/A group rotations have rarely been discussed with respect to the gating coordinate in literature and should be added to the concept of a vibrational TRS.

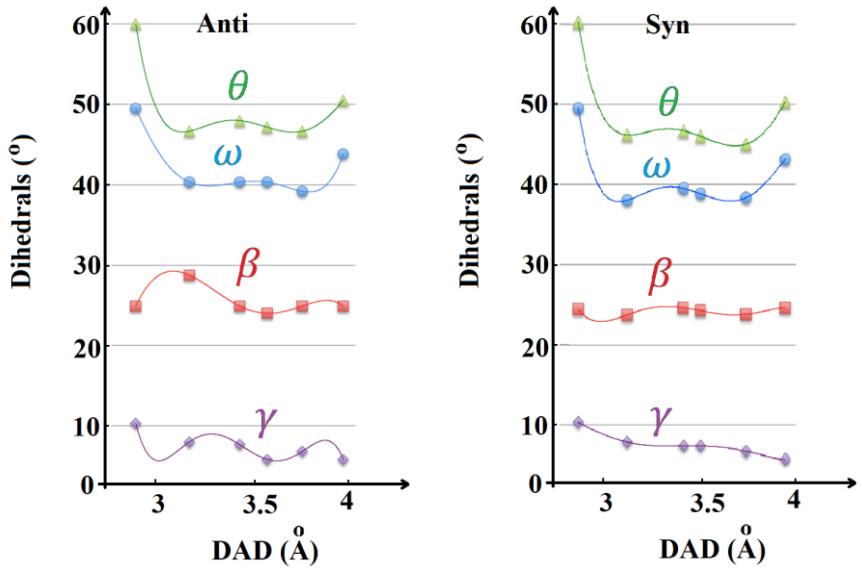

Figure 7. Dihedral angles of the TRS structures as a function of DAD (lines are 6th-order polynomial fit of the results)

Wide range of DADs available to sample, two DAD populations, and prediction of the temperature dependency of 1° KIEs for the reaction of ***1H/1***$^+$

As described in Figure 1, the 1° KIE is related to the ratio of the FC overlap between H *vs.* D transfers. Since the FC overlap ratio increases with increasing DAD, the 1° KIE is larger with TRS's of longer DADs. This explains the usual observation that 1° KIE increases as temperature decreases. With a wide range of DADs (about 2.7 to 4.1 Å) available to sample in this system in gas phase, the 1° KIEs would be extensively temperature-dependent. A close look at the shape of the gating coordinate of this DAD range shows that there are two shallow minima at about 2.9 and 3.9 Å. This suggests that the TRS would have two major DAD populations. In fact, Rosten and Kohen have attempted to fit the temperature dependence of 1° KIEs following the activated H-tunneling model and found that the temperature dependence of the 1° KIEs could be ascribed to two ranges of short and long DADs; and temperature independence of 1° KIEs to only narrowly distributed short DADs.[40] Our results appear consistent with their findings except that the short DAD populations do not refer to a classical TS. This may be true as it is less possible for a single short-lived TRS to sample such a long range of DADs, *e.g.*, from 2.9 to 3.9 Å. Thus, we surmise that two TRS's sample two ranges of DADs but more TRS's sample many small ranges of DADs cannot be excluded. On the other hand, it should be noted that the shape of the gating coordinate may be significantly different compared with the condensed phase. As mentioned in the Introduction, many enzyme-mediated hydride transfer reactions demonstrated temperature independence of 1º KIEs, suggesting narrowly distributed DADs in a rigid active site. Therefore, if the same reaction of **1H**/**1**$^+$ takes place in a space-limited active site of an assumed enzyme, its TRS most likely uses a smaller population of DADs from the gating coordinate in Figure 6.

Concluding remarks

To conclude, we have developed a new approach to compute TRS for hydride tunneling reactions. In the past, freezing the donor-acceptor atoms that gave a fixed DAD was used to compute a TRS, the method developed in this work uses freezing relevant dihedral angles in an assumed initial non-reactive D/A complex and allows the system to optimize its own DAD and conformation. Using the simple self-exchange hydride transfer reaction from isopropyl alcohol to the protonated acetone as an example, the fully-fledged frozen dihedral method was introduced.

The approach was able to be used to search for TRS structures (DADs) from different separations in the initial D/A complexes. The theoretical gating coordinate that correlates the energy of TRS and DAD was given. The whole coordinate is composed of an ensemble of relatively stable TRS structures with DADs from 2.7 to 4.1 Å. Two apparent populations of DADs were found. Formation of a stable TRS of DADs as long as 4 Å is thus possible, although the tunneling efficiency in them is low. Changes in imaginary frequency, ZPE and HOMO orbital for H-tunneling from the D-H$^{\neq}$ to A-H$^{\neq}$ in a TRS were computed, and the nature of the H-tunneling reflected by the change from D-H---A$^{\neq}$ to D---H-A$^{\neq}$ was discussed. We have attempted to apply the method to a mixed hydride transfer system (non self-exchange system) and successfully obtained several TRS structures (see SI). With the TRS structure and the gating coordinate, research is underway to compute both the 1° and 2° KIEs for the hydride transfer reactions.

Acknowledgement: Acknowledgment is made to the donors of the American Chemical Society Petroleum Research Fund (ACS-PRF grant #: 55140-UR4/Lu), the National Science Foundation (NSF# 1800194/Lu), the National Science Foundation for cyberinfrastructure to access the facilities of the Pittsburg supercomputing center (NSF grant #: 1541435), as well as the XSESE startup allocation (CTS170029/Lu) to support the research. The authors also thank Dr. James E. Eilers for the insightful discussions about this research and the manuscript preparation.

Supporting Information: Detailed computational procedures, typical clusters of TRS's optimized from different initial D/A separations, evolution of the HOMO upon C_D-H---$C_A^{\neq}$ transitioning to C_D---H-$C_A^{\neq}$ for a TRS, dynamics that affect the stability of TRS, frequencies of a selected TRS, as well as partial results from the preliminary study of a non self-exchange system.

References:

[1] A. Kohen, in: A. Kohen, H.H. Limbach (Eds.), Isotope effects in chemistry and biology, Taylor & Francis, CRC Press, Boca Raton, FL, 2006, p. 743.
[2] Y. Kim, M.M. Kreevoy, J. Am. Chem. Soc. 114 (1992) 7116.
[3] J.S. Blanchard, W.W. Cleland, Biochemistry 19 (1980) 3543.
[4] S. Hu;, A.V. Soudackov;, S. Hammes-Schiffer;, J.P. Klinman, ACS Catal. 7 (2017) 3569−3574.

[5] C.R.J. Pudney, L.; Sutcliffe, M. J.; Hay, S.; Scrutton N. S. , J. Am. Chem. Soc. 132 (2010) 11329.
[6] J.P. Layfield, S. Hammes-Schiffer, Chem. Rev. 114 (2014) 3466.
[7] B. Maharjan, M. Raghibi Boroujeni, J. Lefton, O.R. White, M. Razzaghi, B.A. Hammann, M. Derakhshani-Molayousefi, J.E. Eilers, Y. Lu, J. Am. Chem. Soc. 137 (2015) 6653
[8] R.P. Bell, The tunnel effect in chemistry, Chapman & Hall, London & New York., 1980.
[9] V. Stojković, A. Kohen, Isr. J. Chem. 49 (2009) 163.
[10] R.J. Harris, Meskys, R., Sutcliffe, M. J., Scrutton, N. S., Biochemistry 39 (2000) 1189.
[11] J. Basran, M.J. Sutcliffe, N.S. Scrutton, J. Biol. Chem. 276 (2001) 24581.
[12] W.A. Francisco, M.J. Knapp, N.J. Blackburn, J.P. Klinman, J. Am. Chem. Soc. 124 (2002) 8194.
[13] M.J. Knapp, J.P. Klinman, Eur. J. Biochem. 269 (2002) 3113.
[14] G. Maglia, R.K. Allemann, J. Am. Chem. Soc. 125 (2003) 13372.
[15] R.S. Sikorski, L. Wang, K.A. Markham, P.T.R. Rajagopalan, S.J. Benkovic, A. Kohen, J. Am. Chem. Soc. 126 (2004) 4778.
[16] L. Wang, N.M. Goodey, S.J. Benkovic, A. Kohen, Philosophical Transactions of the Royal Society B 361 (2006) 1307.
[17] L. Wang, N.m. Goodey, S.J. Benkovic, A. Kohen, Proc. Nat. Acad. Sci. USA 103 (2006) 15753.
[18] Z. Wang, A. Kohen, J. Am. Chem. Soc. 132 (2010) 9820.
[19] V. Stojkoviç, Perissinotti, L., Willmer, D., Benkovic, S., and Kohen, A., J. Am. Chem. Soc. 134 (2012) 1738.
[20] E. Romero, S.T. Ladani, D. Hamelberg, G. Gadda, ACS Catal. 6 (2016) 2113−2120.
[21] Z.D. Nagel, J.P. Klinman, Chem. Rev. 110 (2010) PR41.
[22] S. Hay, M.J. Sutcliffe, N.S. Scruton, in: N.S. Scrutton, R.K. Allemann (Eds.), Quantum Tunnelling in Enzyme-Catalyzed Reactions, RSC Publishing, 2009, p. 199.
[23] A. Kohen, Acc. Chem. Res. 48 (2015) 466.
[24] Q. Liu, Y. Zhao, B. Hammann, J. Eilers, Y. Lu, A. Kohen, J. Org. Chem. 77 (2012) 6825.
[25] S. Kashefolgheta, M. Razzaghi, B. Hammann, J. Eilers, D. Roston, Y. Lu, J. Org. Chem. 79 (2014) 1989.
[26] M. Derakhshani-Molayousefi, S. Kashefolgheta, J.E. Eilers, Y. Lu, J. Phys. Chem. A 120 (2016) 4277−4284.
[27] D. Roston, A. Kohen, J. Am. Chem. Soc. 135 (2013) 13624.
[28] D. Roston, C.M. Cheatum, A. Kohen, Biochemistry 51 (2012) 6860.
[29] J.P. Klinman, A. Kohen, Annu. Rev. Biochem. 82 (2013) 471.
[30] R.L. Redington, C.W. Bock, J. Phys. Chem. 95 (1991) 10284.
[31] Y. Guo, T.D. Sewell, D.L. Thompson, The Journal of Physical Chemistry A 102 (1998) 5040.
[32] R.L. Redington, T.E. Redington, R.L. Sams, The Journal of Physical Chemistry A 110 (2006) 9633.
[33] D. Roston, A. Kohen, Proc. Nat. Acad. Sci. USA 107 (2010) 9572.
[34] Y.P. Liu, D.H. Lu, A. Gonzalez-Lafont, D.G. Truhlar, B.C. Garrett, J. Am. Chem. Soc. 115 (1993) 7806.
[35] Y.P. Liu, G.C. Lynch, T.N. Truong, D.H. Lu, D.G. Truhlar, B.C. Garrett, J. Am. Chem. Soc. 115 (1993) 2408.

[36] C. Alhambra, J.C. Corchado, M.L. Sanchez, J. Gao, D.G. Truhlar, J. Am. Chem. Soc. 122 (2000) 8197.
[37] S.P. Webb, P.K. Agarwal, S. Hammes-Schiffer, J. Phys. chem. B 104 (2000) 8884.
[38] K. Świderek, K. Arafet, A. Kohen, V. Moliner, J. Chem. Theory Comput. 13 (2017) 1375−1388.
[39] P.M. Kiefer, J.T. Hynes, J. Phys. Chem. A 107 (2003) 9022.
[40] D. Roston, C.M. Cheatum, A. Kohen, Biochemistry 51 (2012) 6860.